DIGITAL ACCESS TO SCHOLARSHIP AT HARVARD
DASH.HARVARD.EDU

HARVARD LIBRARY
Office for Scholarly Communication

Cellular Response to Expansion and Compression Forces in Mouse Midpalatal Suture and Surrounding Structures

Citation
Katebi, Negin. 2016. Cellular Response to Expansion and Compression Forces in Mouse Midpalatal Suture and Surrounding Structures. Doctoral dissertation, Harvard School of Dental Medicine.

Permanent link
http://nrs.harvard.edu/urn-3:HUL.InstRepos:33797364

Terms of Use
This article was downloaded from Harvard University's DASH repository, and is made available under the terms and conditions applicable to Other Posted Material, as set forth at http://nrs.harvard.edu/urn-3:HUL.InstRepos:dash.current.terms-of-use#LAA

Share Your Story

The Harvard community has made this article openly available.
Please share how this access benefits you. Submit a story .

Accessibility

Cellular response to expansion and compression forces in mouse midpalatal suture and surrounding structures

A Thesis Presented by

NEGIN KATEBI

To

The Faculty of Medicine

in partial fulfillment of the requirements

for the degree of

Doctor of Medical Sciences

*Research Mentor**: Bjorn Reino Olsen, MD, PhD***
Dean for Research and Professor of Developmental Biology at Harvard School of Dental Medicine
Hersey Professor of Cell Biology at Harvard Medical School

Harvard School of Dental Medicine
Boston, Massachusetts

April 2016

Table of Contents

Abstract

Objectives – To investigate the anatomy of the mouse palate, the midpalatal suture, and the cellular characteristics in the sutures before and immediately after midpalatal suture expansion, and as well as, to study the effects of compression force on the midpalatal suture.

Materials and Methods – Wild-type C57BL / 6 male mice, aged between 6 weeks and 12 months, were chosen for all the experiments. The complete palate of the non-operated group and the midpalatal suture-expanded or -compressed group at different ages was used for histological, micro-CT, immunohistochemistry, and sutural cell analyses. Animals in the experimental group for compression were subjected to palatal suture compression force by closing loops for the periods of 1, 3, 5, 7, 14, and 28 days.

Results – This study documents precise morphological and histological characteristics of the mouse palatal sutures. In addition to the opening of the midpalatal suture caused by expansion, both transverse and interpalatine sutures were also seen to be affected. Cellular density was decreased in different types of sutures following the application of expansion force. In respect to compression study, suture width, maxillary width, and bone volume to total volume were significantly decreased compared to control at 14 and 28 days following the

application of compressive force. Compression force caused an increased cell apoptosis in midpalatal suture area. Osteoclast activity and expression of MMP-9 were increased, specifically on the nasal side.

Conclusions – The detailed morphology and histology of the mouse palate and the cellular changes that occur following midpalatal suture expansion or compression, as described here, will be helpful as a basis for further investigations of palatal suture tissue responses to mechanical force.

Key words: midpalatal suture; collagen II; craniofacial sutures; mechanical force; mesenchymal cell; palate, expansion, compression

This work was supported by research grant R01AR036819 from the National Institutes of Health (to B.R.O.).

Introduction and Review of Literature

Craniofacial sutures and synchondroses are flexible and less stiff than bones. Sutures are dynamic and respond to different types of mechanical stimuli (1). Taking advantage of these properties, orthopedic-orthodontic therapy utilizes applied mechanical stresses to stimulate or inhibit bone growth or to modify direction of growth via changing cellular activities within craniofacial sutures and synchondroses (2).

Understanding the mechanisms by which craniofacial sutures respond to mechanical force is essential for improving orthodontic treatment strategies. Accordingly, scientists are increasingly interested in delineating the events that occur at the cellular and molecular levels during the application of mechanical forces across craniofacial sutures. For half a century the expansion of one such suture, the midpalatal suture, has been successfully used to correct dentofacial deformities and treat maxillary width deficiencies (3). To obtain insights into the basic mechanisms involved, scientists have turned to midpalatal suture expansion in rats and mice. Because of their utility in uncovering genetic mechanisms, mice represent an ideal model for studying the responses of mammalian craniofacial bones and sutures to mechanical forces, and our laboratory has described how an expansive force across the mouse midpalatal suture induces a process of remodeling and regeneration of the suture structure (4). However, further studies of detailed

molecular mechanisms require precise morphological and histological data on the mouse midpalatal suture that are currently unavailable.

Similarly, clinicians have used heavy extra oral (headgear to deliver 500-1000 gram of force per side: 12 hours per day) compressive force in patients with a large dental overjet in order to compress the maxilla. Reduction of maxillary protrusion can be significantly reduced by tipping dentition backward and restricting the skeletal growth of maxilla (20). It has been suggested that compression force can induce bone resorption adjacent to the maxillary circumferential sutures and reduce bone volume (21). While histological analysis in some animal studies show bone resorption and bone displacement (22, 23), others demonstrated that when applying compression force to a suture, rather than resorbing the adjacent bones, they become thickened (24). Therefore, there is no clear answer about how the sutures respond to compression.

Thus, to provide better understanding of both expansion and compression effects on midpalatal suture, first, we have investigated the anatomy of the mouse palate, the midpalatal suture, and the cellular characteristics in the suture before and immediately after midpalatal suture expansion. Second, we looked at the effects of compressive force on histomorphometric values and described how a compressive force across the midpalatal suture of mice induces cell apoptosis, increases the number of osteoclasts and MMP-9 activities which result in bone resorption and reduce bone volume.

Hypothesis and Specific Aims

Hypothesis:

Application of mechanical forces either through expansion or compression to mouse midpalatal suture has no significant cellular effects.

Specific Aims:

Aim 1: To study the mouse palate anatomy in details and look at the sutures' structure at different points of age.

The whole palate of wild-type C56BL/6 male mice, aged between 6 weeks and 12 months old, will be dissected for the study. Each group will consist of at least four mice. Detailed palatal anatomy will be studied by the use of histology analysis and micro CT imaging. Cellular count analysis will be performed on all of the samples to find out the differences within each suture structure and changes that happens with aging.

Aim 2: To study and compare morphological features of the midpalatal suture before and right after mechanical stimuli and study cellular changes from midpalatal suture expansion.

Expansion procedure will be performed on wild type C56BL/6 male animals at 6 weeks of age and two days after the procedure. Samples will be collected and compared to their non-expansion (control or sham) group at five different zones

including midpalatal, transverse palatine and interpalatine sutures. To further evaluate the changes we will perform histochemistry and immunofluorescence labeling.

Aim 3: To study the effects of compressive force on midpalatal suture.

Compression procedure will be performed on C56BL/6 animals at different time periods of 1, 3, 5, 7, and 14 days. Micro-CT analysis will be performed to evaluate midpalatal suture width, maxillary width and bone volume to total volume measurements. Histological analysis (H and E, Saffranin- O staining) will be performed to look at the cellular and structural changes. TUNEL staining will be utilized to visualize the apoptotic cells. Tartrate resistant acid phosphatase (TRAP) staining will be used to evaluate osteoclasts. Moreover, MMP-9 immunohistochemistry will be employed to evaluate changes of MMP-9 expression during the experimental period at different time points.

Materials and Methods

Experimental animals and histological/micro-CT analyses of hard palate

Wild-type C57BL/6 male mice (Charles River Laboratories, Wilmington, MA, USA), aged between 6 weeks and 12 months, were used for all the experiments. Each expansion experimental group consisted of a minimum of four mice. To study the effects of compression, a total of 75 C57BL/6 male mice at six weeks of age were used. The average weight of this group was 22.3 g. Mice at this age have both maxillary first and second molars and they are in a growing phase. Weighting the animals was done at the beginning and the end of the experimental period. 60 animals were divided into 5 experimental groups for histological analysis. They were treated with an applied compression force at different time periods of 1, 3, 5, 7, and 14 days. There were twelve animals for each time point, including six in compression group and six in control group (three sham operated and three non-operated). In addition, fifteen animals were used for micro-CT analysis at 14 and 28 days, including nine animals with compression and six animals serving as controls. The whole palate of each mouse was dissected and fixed overnight with 4% (w / v) paraformaldehyde in 0.1 M phosphate buffer, pH 7.4, demineralized in 0.5 M ethylenediaminetetraacetic acid (EDTA) for 2 weeks at 4°C, and dehydrated in ethanol prior to embedding in paraffin. For histological analysis, 8 μm serial paraffin sections of 6-week-old, 4-, 9-, and 12-month-old mice were cut. Microphotographs were taken (Nikon Eclipse 80i Upright Microscope; Nikon Corporation, Tokyo

Japan) after sections were mounted on the glass slides, de-waxed, and stained with hematoxylin and eosin. Similar steps were followed for histological analysis of mice in compression group at 1, 3, 5, 7, and 14 days. To obtain three- and two-dimensional views of the whole palate, tissues were subjected to high-resolution micro-CT analysis (Xradia MicroXCT system, Pleasanton CA, USA). To obtain three-dimensional views of the palate in compression study group, tissues were subjected to micro-CT analysis (SCANCO μCT 35, Wayne PA, USA). All animal work was performed using protocols approved by the Institutional Animal Care and Use Committee of Harvard Medical School, Boston, MA, USA.

Midpalatal suture expansion & compression procedure

A combination of ketamine (100 mg/ kg) and xylazine (10 mg / kg) was used as anesthetic for the mice. The mice were prepared for midpalatal suture expansion as previously described (4). Briefly, 0.014-in. stainless steel orthodontic wire (GAC International Inc., Bohemia, NY, USA) was used to make opening loops that applied a distracting force across the midpalatal suture. Using a light-cured adhesive (3 M Unitek, Monrovia, CA, USA), the appliances were bonded to first and second maxillary molars on both sides. For sham operation, dead opening loops with no expansion force were prepared and bonded to first and second maxillary molars. For compression experiments, we followed exact same principles but instead of opening the loop, a closing loop was used with the same amount of deflection. Mice were sacrificed after 2 days of midpalatal suture expansion, and the maxilla was

dissected. Cell density in hard palate sutures Hematoxylin- and eosin-stained palates of 6-week-old mice were analyzed for differences in cell density within palatal sutures. Using METAMORPH software (Molecular devices LLC; Sunnyvale, CA, USA), cell density was determined in different regions of the suture. Five different suture zones were chosen, as follows: 1) the midpalatal suture area in the 1st molar tooth region, 2) the midpalatal suture area between the 1st and 2nd molar teeth and between the 2nd molars, 3) the transverse palatine suture area between the 2nd molar teeth and between the 2nd and 3rd molar teeth, 4) the area between 2nd and 3rd molar teeth and the 3rd molar teeth, and 5) the area between the 3rd molar teeth and the interpalatine suture in the posterior region of the palate. The number of cells was determined in the total area of each palatal suture zone (shown in Fig. 2) by counting the number of cell nuclei in the midpalatal area. The final statistical analysis of cell density was based on the number of cells in a 100-μm^2 suture area of each palatal suture zone.

Cell density in hard palate sutures

Hematoxylin- and eosin-stained palates of 6-week-old mice were analyzed for differences in cell density within palatal sutures. Using METAMORPH software (Molecular devices LLC; Sunnyvale, CA, USA), cell density was determined in different regions of the suture. Five different suture zones were chosen, as follows: 1) the midpalatal suture area in the 1st molar tooth region, 2) the midpalatal suture area between the 1st and 2nd molar teeth and between the 2nd molars, 3) the

transverse palatine suture area between the 2nd molar teeth and between the 2nd and 3rd molar teeth, 4) the area between 2nd and 3rd molar teeth and the 3rd molar teeth, and 5) the area between the 3rd molar teeth and the interpalatine suture in the posterior region of the palate. The number of cells was determined in the total area of each palatal suture zone (shown in Fig. 2) by counting the number of cell nuclei in the midpalatal area. The final statistical analysis of cell density was based on the number of cells in a 100-μm^2 suture area of each palatal suture zone.

Histochemistry and immunofluorescence labeling

For apoptosis detection, In Situ Cell Death Detection kit, Fluorescein TUNEL system (Roche Diagnostics, Mannheim, Germany), was used to visualize apoptotic cells. Safranin O/ Methyl Green staining was used to visualize cartilage proteoglycans and bone in frozen and paraffin sections. Briefly, frozen sections were fixed overnight in 4% (w / v) paraformaldehyde in PBS, demineralized in 0.5 M EDTA for 14 days at 4°C, and embedded in Tissue-Tek OCT compound (Sakura Finetek USA, Inc., Torrance, CA, USA) with a slurry of solid CO2 in 95% ethanol. Frozen blocks were sectioned using Leica cryotome (Research Cryostat Leica CM3050 S; Leica Microsystems Inc., Buffalo Grove, IL, USA) and air-dried for 30 min. The 8 µm sections were visualized using a fluorescence microscope (Nikon TE2000w/ C1 Point Scanning Confocal; Japan). For collagen types I and II immunohistochemistry, paraffin sections were deparaffinized and pre-washed prior to enzyme treatments. The tissue sections were digested by sequential treatment with 2 mg /ml of

hyaluronidase (Sigma- Aldrich, St. Louis, MO, USA) in PBS (pH 5.0) for 15 min at 37°C; 250 mU/ ml of chondroitinase ABC (Sigma-Aldrich) in 50 mM Tris, PH 8.0, 60 mM sodium acetate, and 0.02% bovine serum albumin (prepared fresh) for 15 min at 37°C; and finally pepsin (Sigma-Aldrich) at 2 mg / ml in 0.1 M Tris–HCl, pH 2.0 for 15 min at 37°C. After enzyme pretreatments, sections were incubated separately with rabbit polyclonal antibody (Abcam, Cambridge, MA, USA) against collagen type I at 1:100 dilution and mouse monoclonal antibody (Lab Vision, Fremont, CA, USA) against collagen type II at 1:100 dilution overnight. MOM kit (Vector Laboratories, Burlingame, CA, USA) was used to decrease the background staining. Each experimental group consisted of a minimum of four mice with four sections per mouse. To demonstrate acid phosphatase and tartrate resistant acid phosphatase (TRAP) in midpalatal suture, Sigma-Aldrich (St Louis, MO) Acid Phosphatase kit (Procedure No. 387) was used. Steps were followed as recommended by manufacturer. Samples were counterstained with methyl green and mounted with water-based mounting solution.

Immunohistochemistry

MMP-9 expression was examined by immunohistochemistry using anti mouse goat polyclonal MM9 antibody (R&D Systems, inc, Minneapolis, MN). Paraffin sections were deparaffinized and pre-washed prior to antigen retrieval. For antigen retrieval, endogenous peroxidase quenching buffer (3% hydrogen peroxide, normal serum, 10X PBS, and water) was used. Blocking solution contains 1% BSA, 2% normal

serum, and 0.1% Triton X-100. Anti-MMP-9 antibody (ab28364, Abcam, Cambridge, MA) with 1:100 dilution was applied overnight inside humidified chamber at 4°C. After washing with PBS biotinylated secondary antibody was used.

Statistical analysis

Results were presented as mean ± SD. Cell count differences were compared using two-tailed unpaired Student *t* test ($p < 0.05$).

Results

Hematoxylin- and eosin-stained transverse sections of 6-week-old mouse hard palate (Fig. 1A–D) show the presence of three sutures: 1) midpalatal suture (mps) in the middle with a straight shape which narrows down at both poles (Fig. 1A, B), 2) transverse palatine suture (tps) formed as an interlocking joint with a highly complex interdigitated structure (Fig. 1A, C), and 3) interpalatine suture (ips) with an irregular zigzag shape at the posterior end (Fig. 1A, D). Nasal-associated lymphoid tissue (NALT) is prominent between the left and right lateral nasal glands (LNG). The 1st, 2nd, and 3rd molar teeth are seen along the sides of the palate. The bones that meet in midpalatal suture, known as the palatine process of maxilla (ppm), meet in a butt joint. The two halves of the horizontal plates of the palatine bones (p) are joined in the middle at the interpalatine suture and form the posterior section of the hard palate. The occlusal views of the reconstructed hard palate in two- and three dimensional micro-CT images further confirm the histological findings (Fig. 1E, F).

The amount of bone marrow in the bony elements close to the sutures varies in a characteristic fashion. In the midpalatal suture region of the hard palate, bone marrow space is much smaller than in the interpalatine suture area (Fig. 1A, E).

Fig. 1

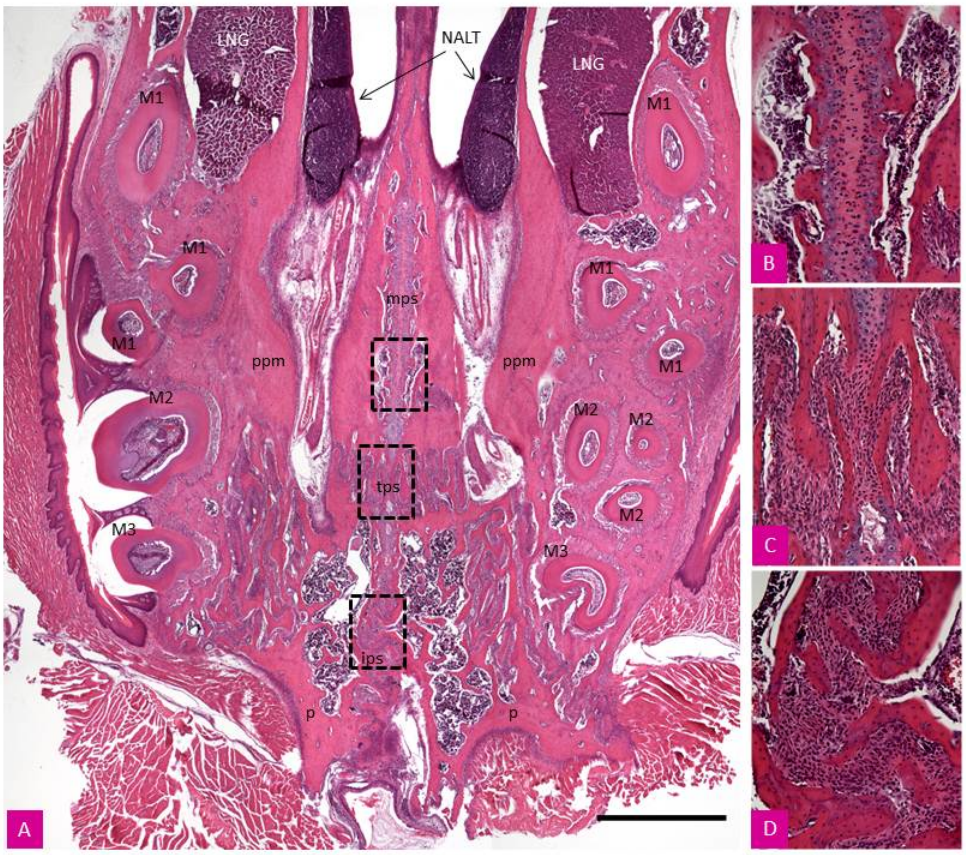
LNG
NALT
LNG
M1
M1
M1
M1
M1
mps
M1
ppm
ppm
M1
M2
M2
M2
tps
M2
M3
M3
ips
p
p
A
B
C
D

Fig. 1 – cont.

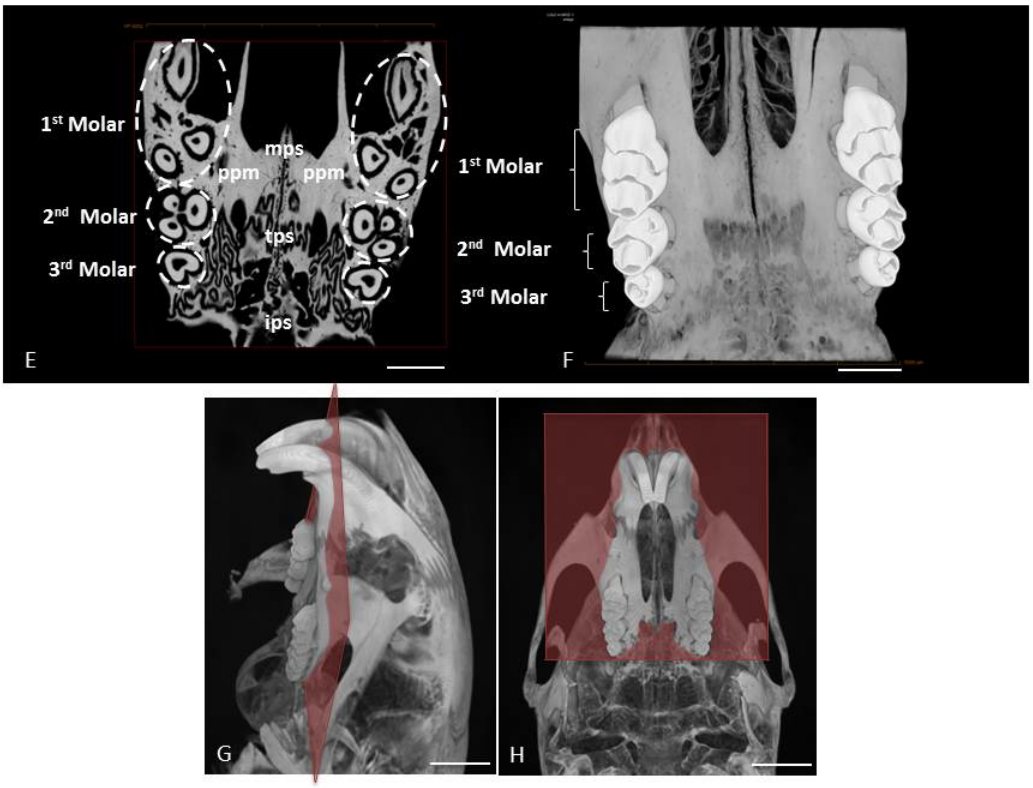

Fig. 1. A transverse section of mouse palate. Hematoxylin and eosin staining of 6-week-old mouse palate (A) with areas of the sutures as indicated by rectangles shown in higher magnification for the midpalatal suture (B), transverse suture (C), and interpalatine suture (D). A micro-CT image of 6-week-old male mouse palate reconstructed in two-dimensional (E) and three-dimensional (F-H) views. The transversal plane is indicated in the mouse palate (G-H). (NALT: nasal associated lymphoid tissue; LNG: lateral nasal gland; M1: 1st molar; M2: 2nd molar; M3: 3rd molar; mps: midpalatal suture; tps: transverse palatine suture; ips: interpalatine suture; p: palatine bone; ppm: palatine process of maxilla). Scale bar (A, E, F): 1000 μm.

This can be clearly seen in frontal sections of the reconstructed micro-CT image of the 6-week-old mouse palate (Fig. 2A1–A5). The small amount of bone marrow close to the transverse suture is similar to that of the midpalatal suture area.

Further histological examination of the midpalatal suture revealed that it mainly consists of secondary cartilage close to the bony edges and with a small amount of fibrous tissue in the central area. From the middle of the sutural gap, a lateral progression of small-sized cells to mature chondrocytes and hypertrophic chondrocytes is evident. The density of cells is notably variable between the different sutures. The posterior part of the hard palate shows the highest density of cells in both the transverse palatine suture and the interpalatine suture in comparison with the midpalatal suture. This was confirmed by morphometric analysis based on examining histological sections (Fig. 2G) as described below.

To study the processes underlying age-related developmental changes in palatal sutures, a series of 6-week-old (Fig. 2B), 4- (Fig. 2C), 9- (Fig. 2D), and 12-month-old mice (Fig. 2E) were used. For the comparison of suture morphology, the palate was divided into five different zones. Starting from the anterior aspect, these zones were 1) the suture between the 1st molar teeth, 2) the suture between 1st and the 2nd molar teeth and between the 2nd molars, 3) the transverse palatine suture between the 2nd molars and between the 2nd and the 3rd molars, 4) the zone between the 2nd and 3rd molars and between the 3rd molars, and 5) the zone between the 3rd molars and the interpalatine suture in the posterior part of the palate (Fig. 2A–F). The most obvious changes because of increasing age were decreasing bone marrow

spaces in the surrounding bones, a reduced number of chondrocytes, a decreasing amount of fibrous tissue between the two cartilaginous regions along the bone margins, a reducing number of periosteal cells in oral and nasal sides, and increased bone formation. Accordingly, the age-dependent progressive ossification in the interdigitated area of the transverse palatal suture results in a more complex structure (Fig. 2B3–E3). In contrast, the midpalatal suture did not ossify during the ages analyzed here. To determine whether the density of cells varied among the different types of sutures, cell nuclei were counted in the five different suture zones in 6-week-old control mice. The data show that there is a significant difference in the cell number per unit area (100 μm^2) among the different suture types. The cell density in the transverse palatine suture and the interpalatine suture was significantly higher than in the midpalatal suture area (Fig. 2G).

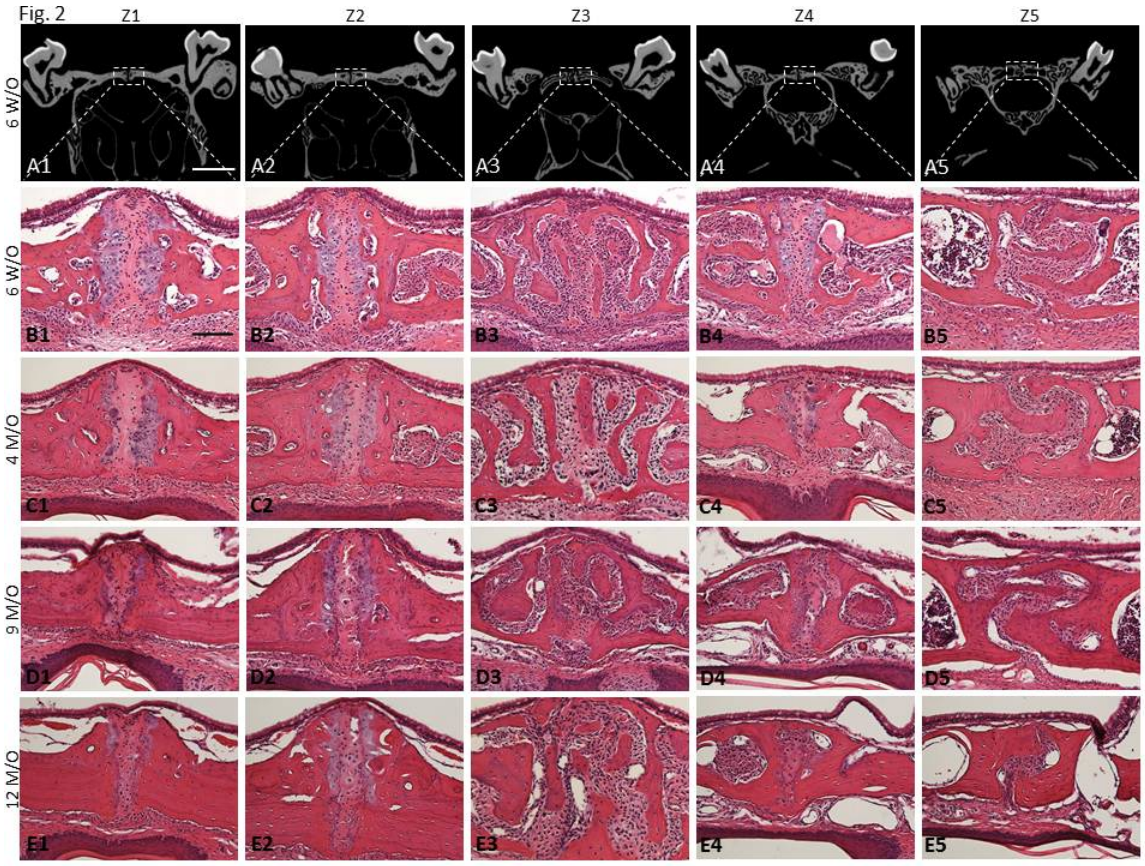

Fig. 2 – cont.

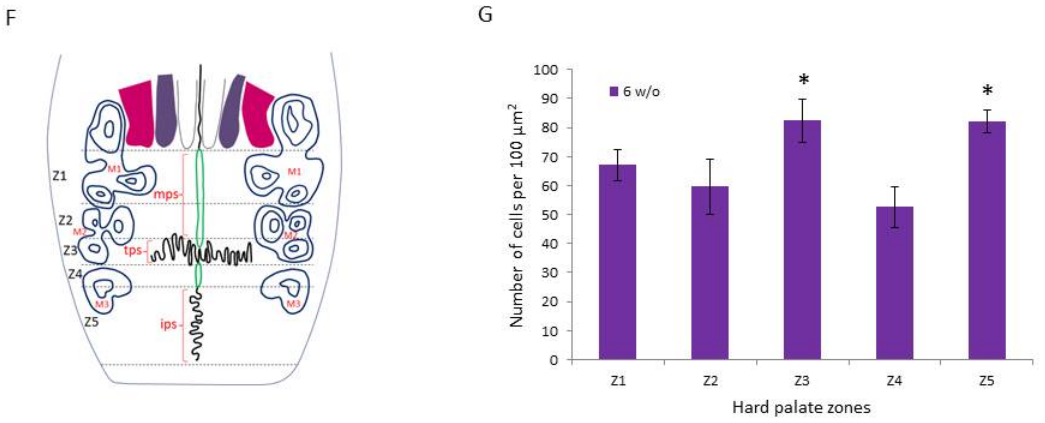

Fig. 2. Frontal section of mouse palate with the nasal side up and oral side down. Micro-CT reconstruction of frontal sections of 6-week-old male mouse palate in two-

dimensional view (A1-A5) and stained with hematoxylin and eosin at different ages of 6 weeks old (B1-B5), 4 months old (C1-C5), 9 months old (D1-D5), and 12 months old (E1-E5) mice are shown. The panels are representative of a series of sections of the palate divided into 5 different zones (see panel F for diagram). Starting from the anterior aspect, these zones are [Z1] the suture between the 1st molar teeth (A1-E1), [Z2] the suture between 1st and the 2nd molar teeth and between the 2nd molars (A2-E2), [Z3] the transverse palatine suture between the 2nd molars and between the 2nd and the 3rd molars (A3-E3), [Z4] the zone between the 2nd and 3rd molars and between the 3rd molars (A4-E4), and [Z5] the zone between the 3rd molars and the interpalatine suture in the posterior part of the palate (A5-E5). The graph (G) represents the cell density in each designated zones of cut sections shown from panels 1-5 of series B (6-week-old mice). The cell density among Z1, Z2, and Z4 zones of midpalatal suture area was not significantly different. However, the cell density in midpalatal suture area was significantly lower in comparison to transverse palatine suture and/or the interpalatine suture ($^{*}p < 0.05$). Scale bar (A1): 1000 μm, (B1): 100 μm.

Effects of Expansion Force

In response to expansive force, the width of the midpalatal suture increased (Fig. 3C). After 2 days of expansion, an increased amount of fibrous tissue and a decrease in the number of chondrocytes was observed. No difference was detected between sham-operated and non-operated mice. Accordingly, these two groups of animals were grouped together as controls. The changes occurring as a result of suture

expansion have been previously published (4). Briefly, the collagen fibers are reoriented across the suture, and periosteal cells migrate into the suture area. Analysis of suture cell counts per unit area (100 μm^2) shows that the cell density is significantly lower in the zones 1–4 of the expanded suture of 6-week-old mice than in control mice of the same age (Fig. 3D). This is primarily the result of expansion of the suture area, although apoptosis, induced by the expansion, contributes as well. The cell number per unit area in zone 5 of expanded palate (interpalatine suture) was lower, but not significant, in comparison with the control group. This may be due to the fact that the interpalatine suture is less affected by the process of midpalatal suture expansion.

Fig. 3

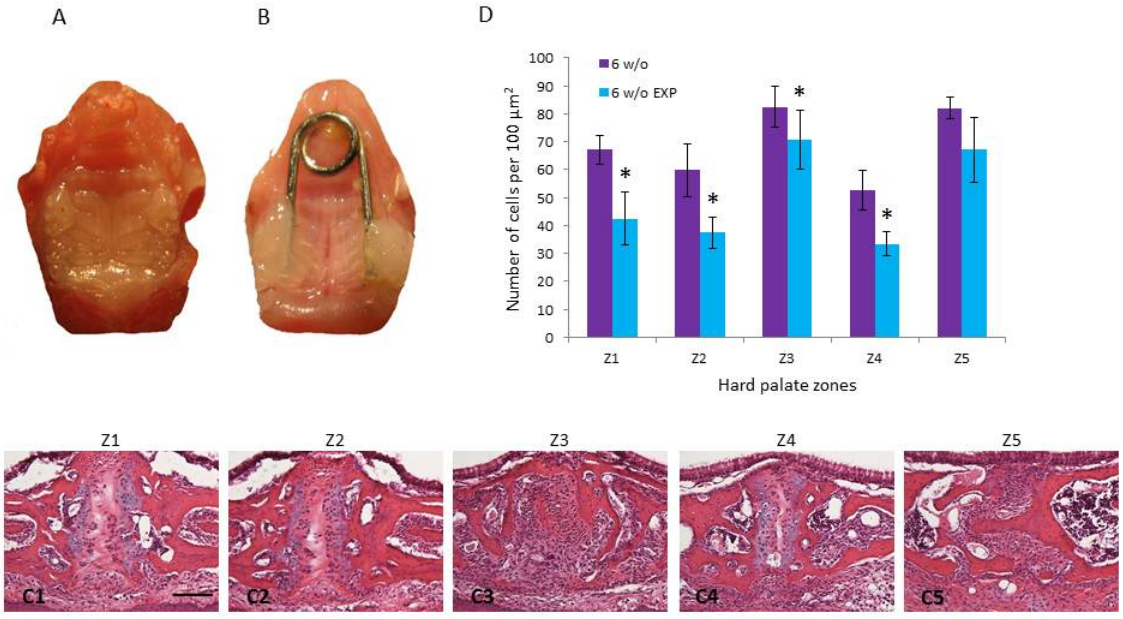

Fig. 3. Midpalatal suture expansion in mouse. Isolated palate of 6-week-old mice is shown with the spring opening loop bonded to the first and second molars (B) versus the non-operated control (A). Hematoxylin and eosin staining of sections of expanded palate of 6-week-old mouse with sections representing the palate divided into 5 different zones. Starting from the anterior aspect, these zones are [Z1] the suture between the 1st molar teeth (C1), [Z2] the suture between 1st and the 2nd molar teeth and between the 2nd molars (C2), [Z3] the transverse palatine suture between the 2nd molars and between the 2nd and the 3rd molars (C3), [Z4] the zone between the 2nd and 3rd molars and between the 3rd molars (C4), and [Z5] the zone between the 3rd molars and the interpalatine suture in the posterior part of the palate (C5). The cell density of expanded palate in zones 1 through 5 of 6-week-old mice compared with same age non-operated control mice (D) was significantly lower (*p <0.05). Scale bar (C1): 100 μm.

To further evaluate and explain the reasons behind the decreased cell density in the midpalatal suture-expanded mice, TUNEL staining for apoptosis of control and expanded midpalatal sutures was performed. Cell proliferation, differentiation, and apoptosis are the key events that occur during tissue remodeling. In control mice, TUNEL-positive cells were mainly seen in the cartilaginous region. In contrast, in the expansion group of mice, TUNEL-positive cells were detected in both periosteal and cartilaginous regions (Fig. 4A–C).

Fig. 4

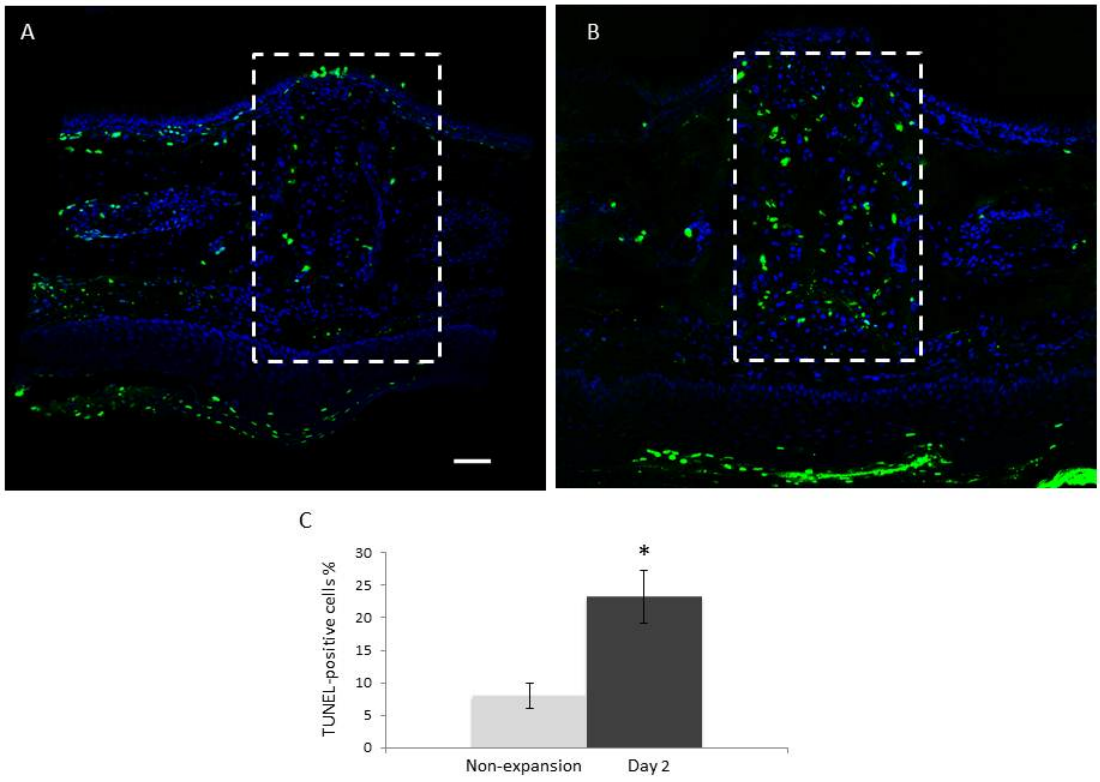

Fig. 4. Increased apoptosis of chondrocytes in expanded midpalatal suture. TUNEL staining of non-operated control (A) and expanded midpalatal suture (B) of 6-week-old mice. After 2 days of midpalatal suture expansion, TUNEL-positive cells (green) were detected in the regions of periosteal cells and chondrocytes within the midpalatal suture area. The percentage of TUNEL-positive cells among the total cells within the midpalatal suture area is compared between control and expansion group (*p <0.05) (Fig. 4C). Scale bar: (A) 100 μm.

Using Safranin O staining, we found that the application of force across the midpalatal suture caused a decrease in the amount of secondary cartilage (Fig. 5).

The significant loss of proteoglycan as judged by decreased Safranin O staining suggests that the tensile force across the suture may induce release and/or activation of matrix-degrading proteases in the suture (Fig. 5B).

Fig. 5

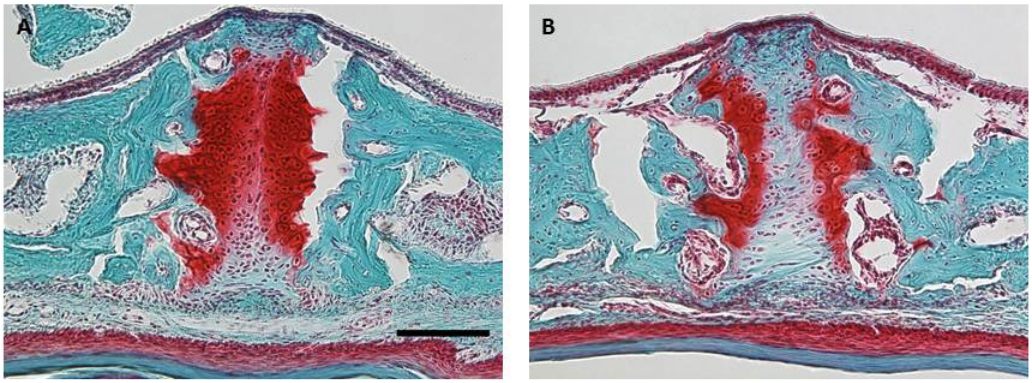

Fig. 5. Safranin O/Methyl Green staining of non-operated control (A) and expanded midpalatal suture (B) of 6-week-old mouse at day 2 of expansion. Scale bar (A): 100 μm.

Finally, collagen I- and II-specific immunofluorescence staining of midpalatal and transverse palatine sutures was conducted. First, analysis of the control group showed that there was an expression of both types of collagen in the midpalatal suture area (Fig. 6A1–A2); further down from the midpalatal area, in the transverse palatine suture, only collagen I staining was detected (Fig. 7A). Of note, the bone matrix in the palatal shelves and periosteal cells on both the oral and nasal sides were clearly stained by collagen I antibodies (Figs 6 and 7). Second, analysis of the

stretched collagen fibers in the midpalatal suture of the expansion group showed mainly the expression of collagen II (Fig. 6B2); however, the matrix surrounding some of the mesenchymal cells in the middle of midpalatal suture area showed the expression of collagen I (Fig. 6B1). In accordance with the results for the control group (Fig. 7A), there was no collagen II expression in the transverse palatine suture of the expansion group; only collagen I was detected (Fig. 7B). The stretched collagen fibers in the transverse palatine area were also stained only with collagen I antibodies (Fig. 7B). Overall, this suggests that the midpalatal suture in mice is more like a fibrocartilage growth region than a collagen I-based fibrous connection between the palatal bones, whereas the transverse palatine area is more like a fibrous suture.

Fig. 6

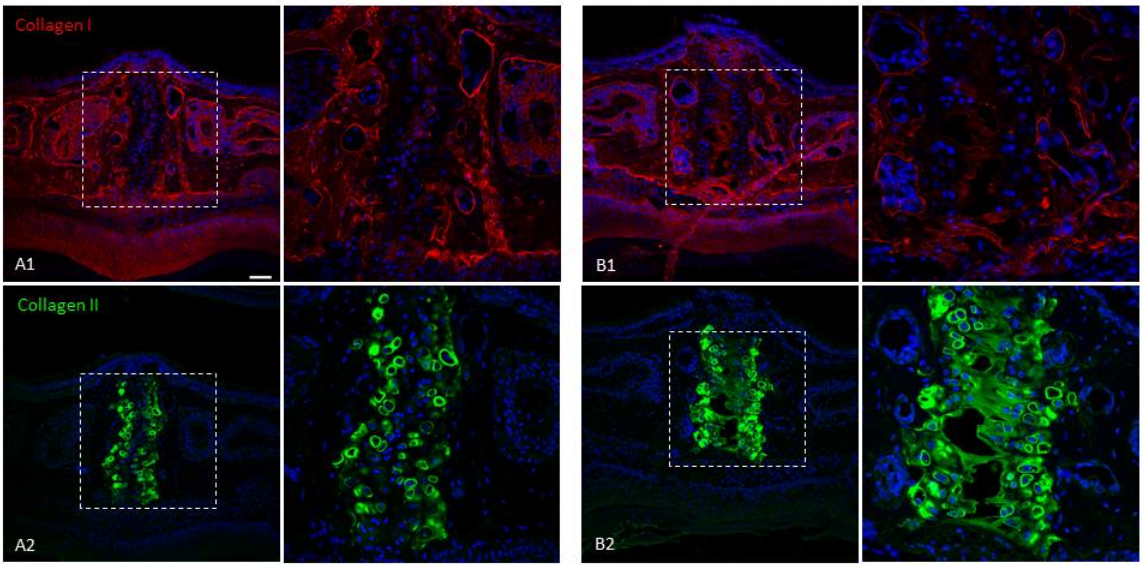

Fig. 6. Confocal images of immunofluorescence staining for collagen I (red) and II (green) of serial palatal sections of non-operated control (A) and expanded midpalatal sutures (B) of 6-week-old mice. After 2 days of midpalatal suture expansion, the stretched collagen fibers in the midpalatal suture area were mostly stained with collagen II-specific antibody. Scale bar (A): 100 μm.

Fig. 7

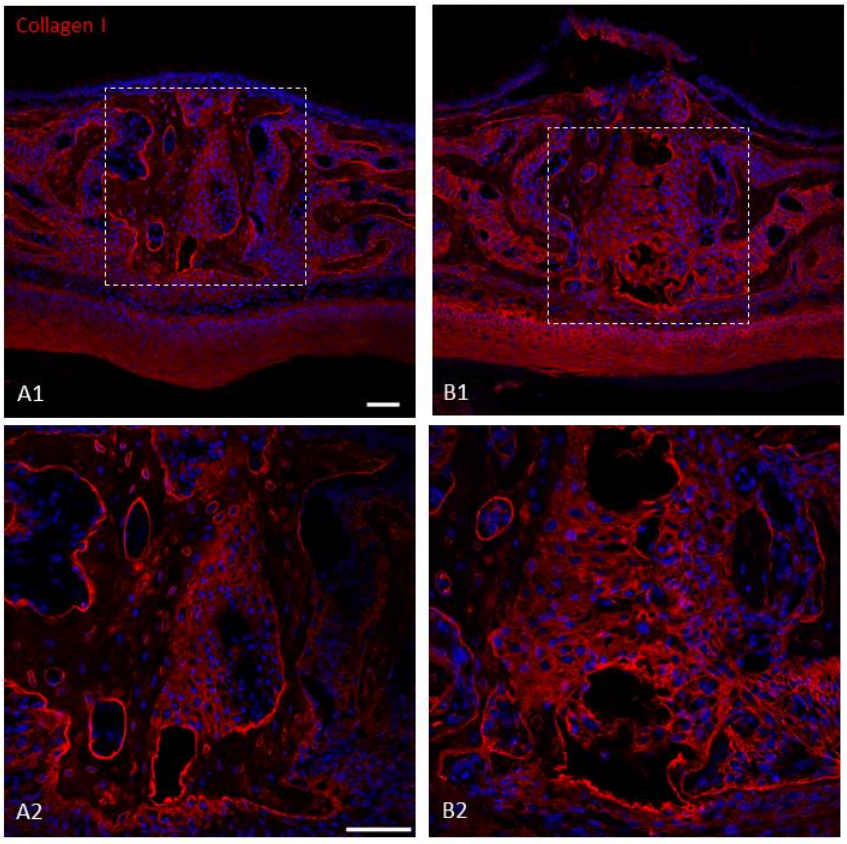

Fig. 7. The collagen I-specific immunofluorescence staining of non-operated control (A) and expanded transverse palatine sutures (B) of 6-week-old mice. The transverse palatine suture area was only stained with collagen I-specific antibody in both the non-operated and expansion groups. Scale bar (A1, A2): 100 μm.

Effects of Compression Force

In this part of the study midpalatal sutures of C57 BL/6 male mice were used to evaluate the possible consequences after applying compression force at different time points. The photographs (Fig. 8) were taken from the whole palate of mice in control group (Fig. 8A) and compression group at day 1 (Fig. 8B), day 3 (Fig. 8C), day 5 (Fig. 8D), day 7 (Fig. 8E) and day 14 (Fig. 8F). Review of morphological comparison between different days reveals a gradual shortening of width of the palate and the distance between molars at each higher time point of the experiment.

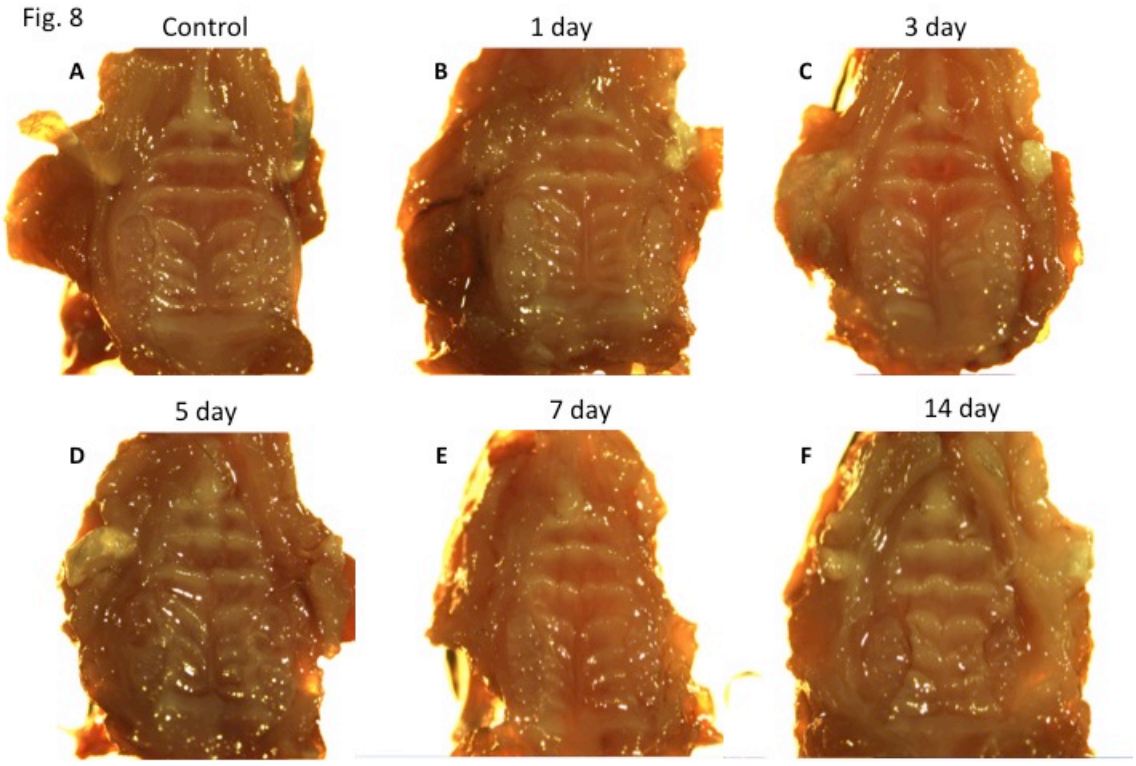

Fig. 8. Midpalatal suture compression in C57 BL/6 mice. Occlusal views of hard palate in

6-week-old mice without compression (A), and with compression at 1 day (B), 3 days (C), 5 days (D), 7 days (E) and 14 days (F).

The body weights of mice were decreased in both compression and sham operated (dead opening loops) groups on days 1, 3, 5 and 7 (Fig. 9, $p<0.05$) compared to control groups (blue line). Since the loops are bonded to first and second maxillary molars, food intake is most likely disturbed. While the sham-operated (green line) groups recover after 7 days, the compression group (red line) did not recover completely even after 28 days. No significant difference in body weights between sham-operated and non-operated mice was observed at days 14 and 28. Although this was not desired, some of the changes following application of compression force might be caused by systemic physiological reactions to the applied force.

Based on micro-CT analysis, a significantly decreased width of midpalatal suture on the oral third ($p<0.05$) was observed at day 14 and day 28 of the experimental group compared to controls. Both nasal third and middle third had a decrease in width, too. However, these numbers are not statistically significant at those sites. Moreover, there is a decrease of about 20% in maxillary width at day 14 and approximately 33% decrease of maxillary width ($p<0.001$ for both) at day 28 in compression group (Fig. 10 and Table 1).

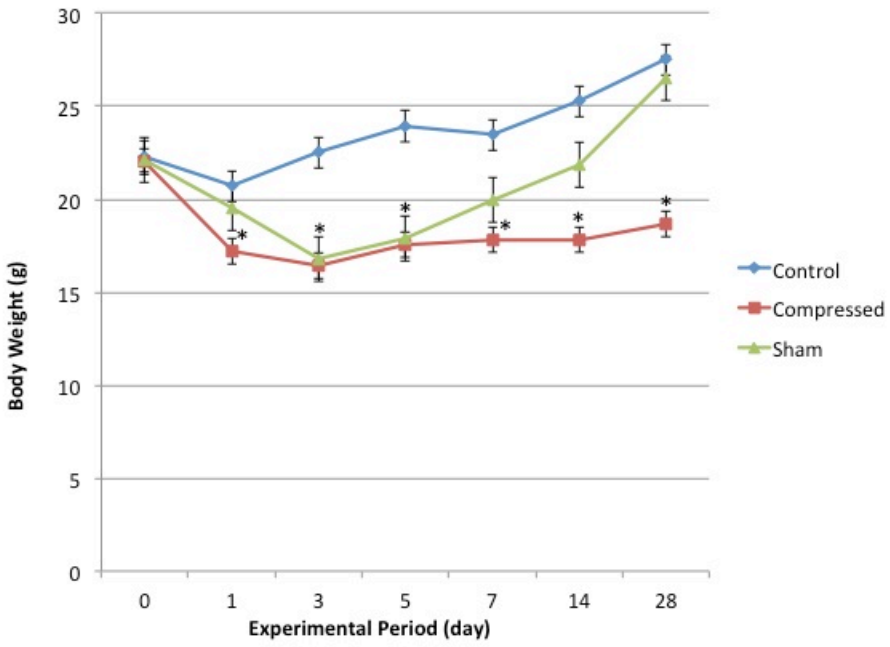

Fig. 9. Body weight changes during experimental period. Body weight curves of non-operated (blue line), sham-operated (green line) and compression group (red) animals. The body weights of compression and sham-operated animals were statistically lower than the control (non-operated) groups at day 1,3, 5, and 7 ($*p<0.05$). The animals in a sham group recovered their body weight by 14 days. However, body weight of experimental group remained lower at 14 and 28 days.

The Bone Volume to Total Volume (BV/TV) measurements were used to look at the overall changes in palatal bones. Changes in the size of bone marrow cavities are reflected in changes of BV/TV since the total volume was defined by outlining the palatal bones. The BV/TV significantly decreased in both day 14 and day 28 of compression groups from 38.3±0.9% to 16.4± 0.4% and from 37.4±1.1% to 15.7±0.5% ($p<0.05$ for both) (Table1).

Table 1. Histomorphometric measurements from mice in experimental group and their controls

Duration	Group	No. of mice	Suture width (mm)			Maxilla width (mm)	BV/TV (%)
			Nasal third	Middle third	Oral third		
14 Days	Control	3	0.061 ± 0.019	0.055 ± 0.010	0.114 ± 0.025	2.706 ± 0.067	38.3 ± 0.097
14 Days	Compression	4	0.058 ± 0.015	0.046 ± 0.015	0.068 ± 0.022*	2.197 ± 0.180**	16.4 ± 0.042*
28 Days	Control	3	0.053 ± 0.010	0.050 ± 0.008	0.099 ± 0.006	2.726 ± 0.031	37.4 ± 0.114
28 Days	Compression	5	0.040 ± 0.025	0.038 ± 0.026	0.057 ± 0.025*	1.807 ± 0.263**	15.7 ± 0.059*

BV/TV, bone volume/total volume.Results are presented as mean ± SD, *p<0.05 compared with control, **p<0.001 compared with control

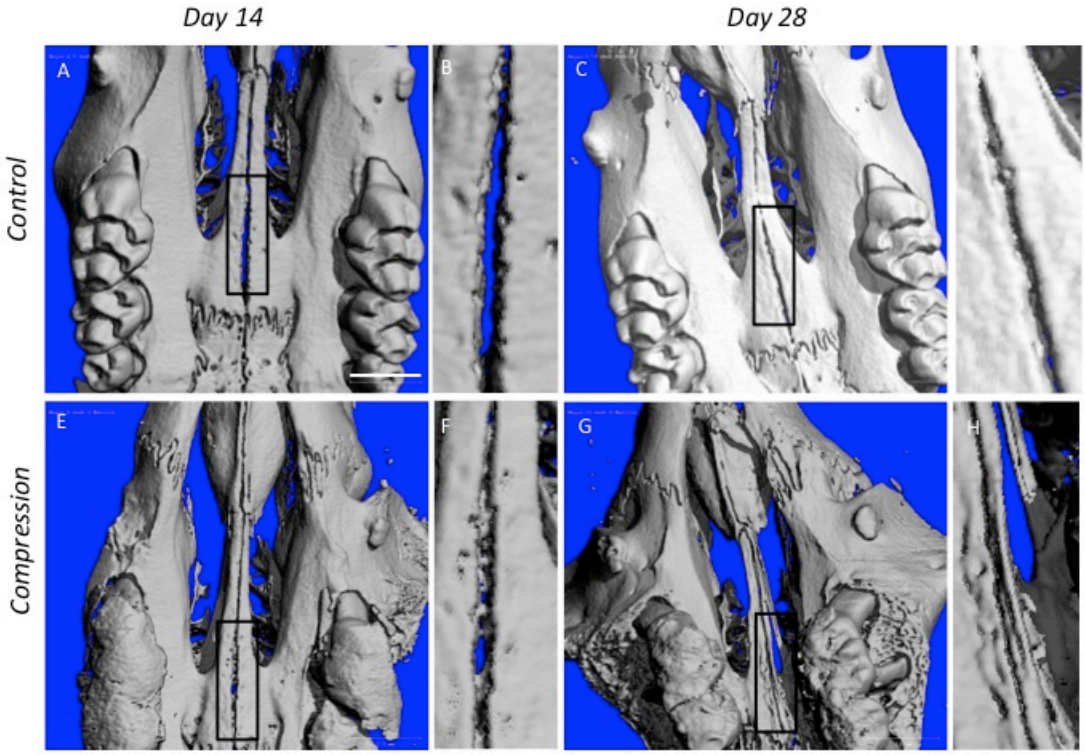

Fig. 10. Three-dimensional micro-CT reconstruction of control and compression maxillae. Occlusal view of reconstructed maxillae of control (A–D) and compression (E–H) animals at day 14 (A, B, E and F) and day 28 (C, D, G and H). Panels B, D, F and H

are high magnification images of the areas marked by rectangles in panels A, C, E and G, respectively. (E and G) Rectangle marks the compressed suture area; the suture is narrower. Scale bar (A): 1.0 mm.

Histological analysis was used to study the changes of suture morphology in response to compression. Since there was no overall histology difference between non-operated groups and sham-operated groups, we grouped them together as controls. As it was described earlier, even though the suture in control group would go through minor changes due to normal growth, the overall width would remain steady during the experimental period. The effects of compression can be observed from day 1 following the placement of the closing loop (Fig. 11B).

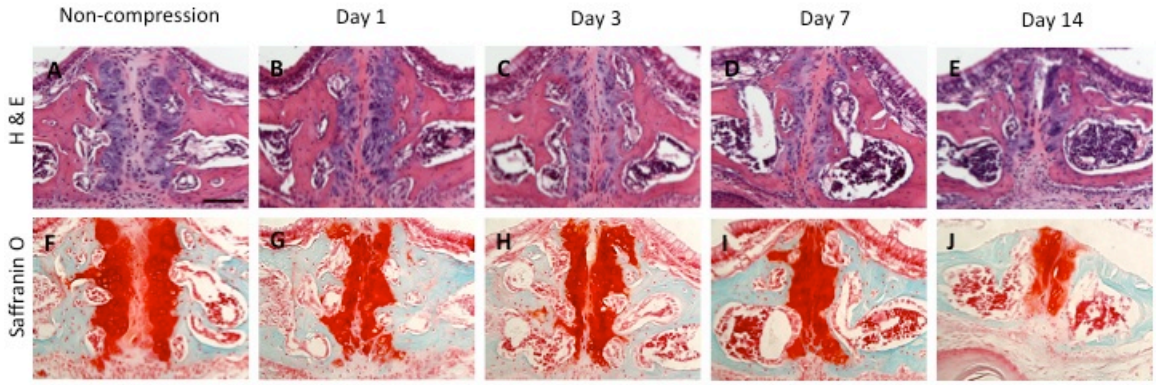

Fig. 11. Effects of midpalatal suture compression on C57 BL/6 mice. Hematoxylin and eosin (A–E) and saffranin O/Methyl Green (F–J) staining of frontal sections of midpalatal sutures of animals without compression (A and F) and with compression at days 1 (B and G), 3 (C and H), 7 (D and I) and 14 (E and J). All the images in this figure and following figures are oriented with nasal side up and oral side down. Scale bar (A): 100 μm.

The distance between the two masses of chondrocytes that are covering the edges of palatal bones are getting smaller during the experimental period from day 1 to day 14 (Fig. 11 B-D) compared to control (Fig 11. A). Bone marrow spaces close to midpalatla suture area got larger after application of compression force (compare Fig. 11A with Figs. 11 B-E). Saffranin O/ Methyl Green staining showed that the amount of cartilage in the midpalatal suture got gradually decreased in the experimental animals (Fig 11G-J) in comparison to control group (Fig 11F). Even one day after the application of compression force the proteoglycan content got changed (Fig 11G) and became less pronounced.

Fig. 12

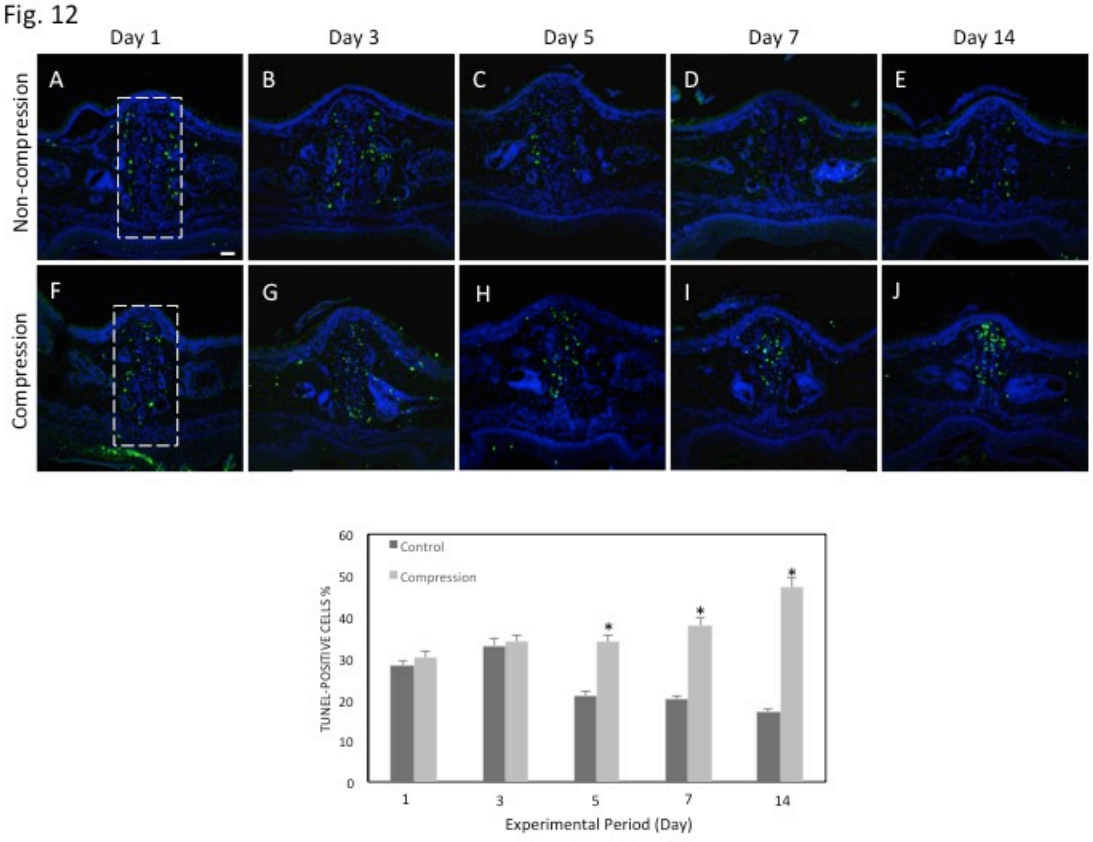

Fig. 12. Increased cell apoptosis in midpalatal suture of C57 BL/6 mice in response to compressive force. TUNEL staining of frontal sections of midpalatal sutures of animals without compression (A–E) and with compression (F-J) from days 1 (A, F), 3 (B, G), 5 (C, H), 7 (D, I), and 14 (E, J). The percentage of TUNEL-positive cells among the total cells within the midpalatal suture area is compared between control and compression group at each specific time point (*p <0.05) (Fig. 12K). Scale bar (A): 100 μm

The most dramatic change in the amount of proteoglycan content can be observed at day 14 which became much less compared to control (Compare Fig 11F with Fig. 11J). Based on both Micro-CT and histology analysis the width of the midpalatal suture got decreased. To further analyze the reasons behind this reduction, TUNEL staining for apoptosis of control and compressed midpalatal sutures was performed at different time points (Fig. 12). In both control and compression groups most of apoptotic cells were located in the midpalatal suture area. Number of positive apoptotic cells got gradually increased with the pick at day 14. There was no statistically significance difference between the numbers of apoptotic cells at day 1 and day 3 (Fig. 12A-B, F-G). However, starting from day 5, day 7 and day 14, there was a statistically significant difference between the number of apoptotic cells between control and operated groups (Fig. 12C-E, H-J). In addition, immunohistochemistry staining of MMP-9 antibody was performed. Analysis of the control group showed that there was an expression of MMP-9 in the bone marrow area and nasal side of the midpalatal suture (Fig. 13A). In the experimental group

the MMP-9 was detected in the same areas as control, however, the staining got intensified from day 1 to day 14 on the nasal side (Fig. 13A-E). Moreover, on day 7 and day 14 there was a continuous line (coming from right and left side of the midpalatal suture area) of expression on the nasal side, including periosteal cells on that side (Fig 13D-E).

Fig. 13

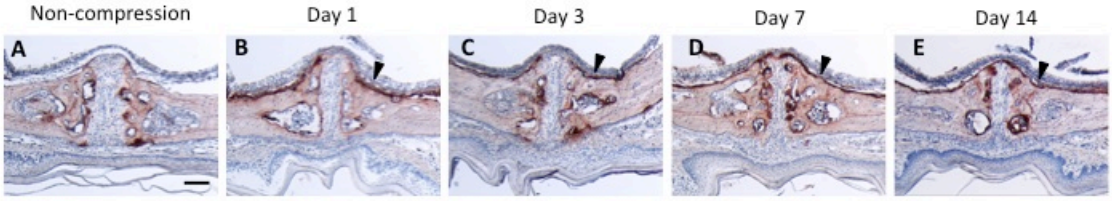

Fig. 13. Expression of matrix metalopeptidase 9 (MMP-9) on nasal side of midpalatal suture. Frontal sections of midpalatal sutures of control (A) and compression animals at days 1 (B), 3 (C), 7 (D), and 14 (E). Sections were stained with MMP-9 antibody (A-E). Filled arrows point to increased MMP-9 antibody staining on the nasal side of the midpalatal suture in the experimental group (B-E). Scale bar (A): 100 μm.

Finally, TRAP staining was performed to detect the osteoclasts. Although TRAP-positive multinucleated cells were present both on control (Fig 14A) and compression groups on day 7, the osteoclasts seemed to have more pronounced presentation on the nasal side of the midpalatal suture.

Fig. 14

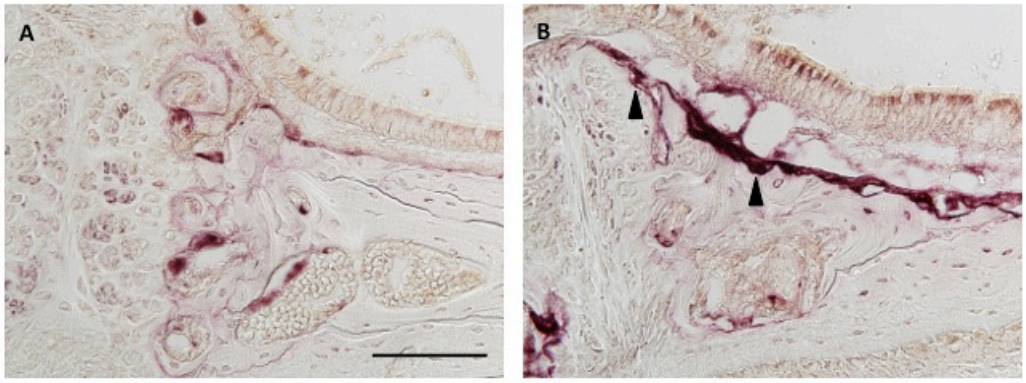

Fig. 14. Increased osteoclast activity in compression suture. Frontal sections of midpalatal sutures of control animals at day 7 (A) and compression animals at day 7 (B). Sections were stained for tartrate-resistant acid phosphatase (TRAP). (B) Arrows point to osteoclasts on the nasal side of the palatal bone surfaces (E) and on the surface of bone marrow cavities (F). Scale bar (A): 100 μm.

Discussion

The aims of the present study were to investigate the anatomy of the mouse palate at different ages, compare morphological features of the midpalatal suture before and right after mechanical stimuli, and study cellular changes resulting from midpalatal suture expansion or compression. The study documents that the midpalatal suture in mice mainly consists of secondary cartilage with collagen II rich fibrous connective tissue in the central area between two cartilaginous regions.

As in many other anatomical aspects in mice and humans, the palatal structure of the two species shows similarities. Both human and mouse osseous palates consist of the horizontal processes of the palatine bone posterior to the transverse palatine suture and the palatine processes of the maxillary bone anterior to that suture. Both bones are joined by sutures which are arranged in two anatomical planes, the transverse and sagittal. This structure allows the palate to grow in two directions, elongate in the antero-posterior direction and widen in the lateral direction (2, 5). While the trigger for widening growth originates from inside the sagittal midpalatal and interpalatine sutures, the transverse palatine suture functions as a growth center for antero-posterior elongation (6).

While mice and humans share similarities in the anatomy of palatal sutures, there are some notable differences. Palatal growth and suture morphology in humans were investigated by Melsen from birth to adulthood (7). Three stages were shown in the Melsen study: in the infantile period the suture was broad and Y-shaped; in

the juvenile period the suture was longer in the vertical aspect and started to become interdigitated; and finally, in the adolescent stage the suture was very tortuous with increased interdigitation. (7). However, the midpalatal suture in adult mice is a straight line between the palatal bones while in humans it forms an interdigitated structure. Another difference is the presence of secondary cartilage in the mouse and the absence of it in humans. Previous studies in rodents have shown that secondary cartilage only forms in response to mechanical stimulation (8, 9). It has also been reported that the type of stimulation makes a significant difference in the outcome. While mechanical tension combined with hyperoxia can boost mesenchymal cell differentiation into osteoblasts, mechanical stress combined with ischemia and hypoxia can favor differentiation into chondroblasts (10, 11). Another factor that can affect the development of sutural cartilage is the masticatory forces which are quite different between mice and humans (12). Accordingly, changes in various forces during craniofacial growth and development, and differences in the masticatory forces, dentition, and occlusion between mice and humans, are likely among the reasons for the presence of secondary cartilage in mice and the absence of it in humans.

In mammals, the sutures are considered to be fibrocellular tissues which are adapted to various types of strain that are different in pattern and magnitude (1). In children and youngsters with cases of transverse maxillary hypoplasia, rapid maxillary expansion (RME) is chosen as a treatment option (3, 13). When RME is performed in the human palate, the opening of the midpalatal suture is not the only

effect. In fact, the circumaxillary sutures separating maxilla from adjacent facial bones are also affected (14). As a result, they show bony displacement responses which are highly variable among sutures (15). Different structures of the skull, including the nasal septum, experience various stresses applied during midpalatal suture expansion (16). As previously described, the study of *Wnt1Cre;Pkd1* mice showed that the nasal cartilage, one of the surrounding areas of the midpalatal suture, experienced abnormal ossification during postnatal development and in response to midpalatal suture expansion (17). In our present study, both transverse and interpalatine sutures also seen to be affected during midpalatal suture expansion. The decreased cell density in different types of sutures of the expansion group versus the control group of mice is likely a consequence of the diverse effects of the midpalatal suture expansion procedure. These effects are likely to be more absorbed by the midpalatal area than the interpalatine suture area. Although the density of mesenchymal cells in the interpalatine suture of expansion mice was slightly lower in comparison to the control group, the difference was not statistically significant. This is an indication of the smaller effect of midpalatal suture expansion on the posterior hard palate. In addition, the apoptosis measurements showed an increased number of TUNEL-positive cells in the midpalatal suture area. However, differences in cellular density are not only based on the role of apoptosis of cells but are also correlated with the size of the matrix space. As the matrix area increases due to expansion, some of the cells die while the remaining cells are scattered around. As a result, the density of cells in the midpalatal suture area decreases. On

the other hand, the decreased density of mesenchymal cells in the transverse palatine and interpalatine sutures is mainly because of dispersion of cells due to the force-induced increase in the suture matrix space.

The spheno-occipital synchondrosis plays a major role in growth of the cranial base (18). In the study of Cendekiawan et al. (19), it was shown that mechanical tension stimuli increased the expression of collagen type II in the spheno-occipital synchondrosis of mice (19). Thus, we speculate that the collagen type II expression in the expanded midpalatal suture of mice may be the result of stretching the suture tissue. Additionally, the collagen I expression in the matrix surrounding mesenchymal cells residing in the expanded midpalatal suture area may be an indication that these cells are differentiating osteoblasts. Such collagen I expressing cells was also found among the periosteal cells on both the oral and nasal sides of the suture.

In regards to compression study, progressive bone resorption altered suture width, maxillary width, and the bone volume to total volume ratio at 14 and 28 days following the application of compressive force. These results confirmed the previously published *in vivo* studies (22,23), that bone resorption was observed following application of compressive force.

Moreover, Increased bone remodeling activity can be speculated based on the fact that our micro-CT results showed increased bone marrow spaces at days 14 and 28. In agreement to that, the number of osteoclasts along palatal bone of nasal side and along the surfaces of bone marrow spaces was seen to be significantly increased. In

addition, it is shown in Fig. 12 that the number of apoptotic cells were increased which can contribute to the fact that the midpalatal suture width is decreased. Matrix metalloproteinases (MMPs) are a group of enzymes that are responsible for degrading extracellular matrix (25). It was shown in the study by Liu Y et al that MMP-1 and 13 expression got intensifies following the application of compression force. (26). In this study we looked that expression of MMP-9. Interestingly, MMP-9 was highly expressed in the exact same areas as osteoclasts which was along the nasal side of the palatine bone and around the bone marrow cavities. This is not surprising since it has been shown that MMP-9 is highly expressed in multinucleated osteoclasts (27).

In summary, a schematic model represented in Fig. 15, describes the activities which occur during midpalatal suture expansion and/or compression. While some factors contribute in inhibiting osteogenesis and chondrogenesis, some factors contribute in promoting osteogenesis and chondrogenesis.

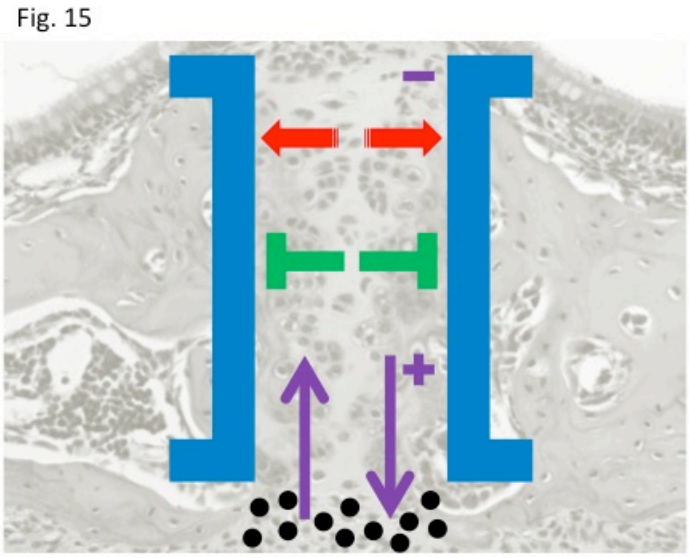

Fig. 15. A model representing the activities occurring during midpalatal suture expansion or compression. (+): osteoblastic activities, (-): osteoclastic activities.

Conclusions

This study suggests that the midpalatal suture in mice is more like a fibro-cartilage growth region than a collagen I-based fibrous connection between the palatal bones. In contrast, the transverse palatine area is more like a fibrous suture. Furthermore, we described the morphological and histological properties of the mouse midpalatal suture in detail. This will serve as the basis for further studies of the molecular and cellular mechanisms involved in suture development and responses to mechanical manipulation. We provided evidence that compression force could result in reduced bone volume and/or bone resorption. Understanding these mechanisms will be required for improving the clinical outcomes of orthopedic–orthodontic therapies in human patients.

Clinical relevance

There are notable similarities and differences in the anatomy of palatal sutures between mice and humans. For half a century, the midpalatal suture expansion technique has been widely used to correct dentofacial deformities and treat maxillary width deficiencies in humans. Moreover, headgear has been used to inhibit maxillary growth by applying compression force via the molars and the alveolar bone However, the cellular and molecular mechanisms underlying the responses of suture tissue to mechanical forces have not been fully understood. This study provides the basis for the experimental work in mice that will be needed for improving the clinical outcomes of orthopedic orthodontic therapies in human patients.

References

1. Herring SW. Mechanical influences on suture development and patency. *Front Oral Biol* 2008;12:41–56.

2. Yu HS, Baike HS, Sung SJ, Kim KD, Cho YS. Three-dimensional finite-element analysis of maxillary protraction with and without rapid palatal expansion. *Euro J of Orthod* 2007;29:118–125.

3. Haas AJ. Rapid expansion of the maxillary dental arch and nasal cavity by opening the mid-palatal suture. *Angle Orthod* 1961;31:73–90.

4. Hou B, Fukai N, Olsen BR. Mechanical force-induced midpalatal suture remodeling in mice. *Bone* 2007;40:1483–1493.

5. Raisz LG. Physiology and pathophysiology of bone remodeling. *Clin Chem* 1999;45:1353–8.

6. Silau AM, Nijo B, Solow B, Kjaer I. Prenatal sagittal growth of the osseous components of the human palate. *J Craniofac Gen Dev Biol* 1994;14:252–256.

7. Melsen B. Palatal growth studied on human autopsy material. *Am J Orthod* 1970;68:42–54.

8. Yu JC, Wright R, Williamson MA, Braselton JP, Abell ML. A fractal analysis of human cranial sutures. *Cleft Pal-Craniofac J* 2003;40:409–415.

9. Alaqeel SM, Hinton RJ, Opperman LA. Cellular response to force application at craniofacial sutures. *Orthod Craniofacial Res* 2006;9:111–122.

10. Hall BK. Cellular differentiation in skeletal tissues. *Biol RevCamb Philos Soc* 1970;45:455–484.

11. Rice DP. Developmental anatomy of craniofacial sutures. In: Rice DP, editor. Craniofacial sutures. Development, Disease and Treatment. Front Oral Biology. Basel: Karger; 2008. vol 12 p. 1–21.

12. Hinton RJ. Response of the intermaxillary suture cartilage to alterations in masticatory function. *Anat Rec* 1988;220:376–87.

13. Suri L, Taneja P. Surgically assisted rapid palatal expansion: A literature review. *Am J Orthod Dentofacial Orthop* 2008;133:290–302.

14. Leonardi R, Sicurezza E, Cutrera A, Barbato E. Early post-treatment changes of circumaxillary sutures in young patients treated with rapid maxillary expansion. *Angle Orthodontist* 2011;81:36–41.

15. Sun A, Hueni S, Tee BC, Kim H. Mechanical strain at alveolar bone and circummaxillary sutures during acute rapid palatal expansion. *Am J Orthod Dentofacial Orthop* 2011;139:219–228.

16. Jafari A, Shetty KS, Kumar M. Study of stress distribution and displacement of various craniofacial structures following application of transverse orthopedic forces--a three-dimensional FEM study. *Angle Orthodontist* 2003;73:12–20.

17. Hou B, Kolpakova-Hart E, Fukai N, Wu K, Olsen BR. The polycystic kidney disease 1 (Pkd1) gene is required for the responses of osteochondroprogenitor cells to midpalatal suture expansion in mice. *Bone* 2009;44:1121–1133.

18. Tang M, Mao JJ. Matrix and gene expression in the rat cranial base growth plate. *Cell Tissue Res* 2006;324:467–474.

19. Cendekiawan T, Wong RW, Rabie AB. Temporal expression of SOX9 and type II collagen in spheno-occipital synchondrosis of mice after mechanical tension stimuli. *Angle Orthodontist* 2008;78:83–88.

20. Armstrong MM. Controlling the magnitude, direction, and duration of extraoral force. *Am J Orthod* 1971;59:217-43.

21. Gautam P, Valiathan A, Adhikari R. Craniofacial displacement in response to varying headgear forces evaluated biomechanically with finite element analysis. *Am J of Orthod Dentofacial Orthop* 2009;135:507-15.

22. Tuenge JRERH. Cephalometric and histologic changes produced by extraoral high-pull traction to the maxilla in Macaca mulatta. Am J Orthod 1974;66:599-617.

23. Meldrum RJ. Alterations in the upper facial growth of Macaca mulatta resulting from high-pull headgear. Am J Orthod 1975;67:393-411.

24. Kopher RA, Mao JJ. Suture growth modulated by the oscillatory component of micromechanical strain. J Bone Miner Res 2003;18:521-8.

25. lgren J, Maisi P, Sorsa T, Sutinen M, Tervahartiala T, Pirila E, et al. Expression and induction of collagenases (MMP-8 and -13) in plasma cells associated with bone destructive lesions. J Pathol 2001;194:217-24.

26. Liu Y, Song F, Sun J, Yu H, Liu SS. Suture compression induced bone resorption with intensified MMP-1 and 13 expressions. Bone. 2012 Oct;51(4):695-703.

27. Vu TH, Werb Z. Matrix proteinases: effects of development and normal physiology. Genes Dev. 2000 Sep 1;14(17): 2123-33.